

Experimental Investigation of Local Film Thickness and Velocity Distribution Inside Falling Liquid Films on Corrugated Structured Packings

Sören J. Gerke*, Hannes Leuner, Jens-Uwe Repke

Technical University of Berlin, Process Dynamics and Operations Group, Straße des 17. Juni 135, 10623 Berlin, Germany
soeren.j.gerke@tu-berlin.de

Understanding the complex fluid dynamics of the liquid phase in structured packing is crucial for the prediction of the separation performance of packed tower and for further optimization of the packing geometry. Detailed numerical investigations are useful to study a wide range of parameters, but require high computational effort and validation is required. Therefore, in this study, experimental investigations on the gravity driven liquid film flow phenomena over corrugated structured packing geometries are presented and evaluated. Due to the fragile nature of thin liquid films, nonintrusive optical measurements were performed through the backside of transparent moldings of packing geometries, thereby reducing optical distortion. To enable the investigation of three-dimensional flow phenomena a μ -Stereoscopic Particle Image Velocimetry (μ SPIV) was adapted for thin liquid films. Measurements are performed on MONTZ-Pak B1.250 macro-structure with a smooth surface or a micro-structured surface at different locations. Values of film thicknesses and velocity distributions inside the falling liquid film are discussed in detail.

1. Introduction

Structured packings are used in columns for distillation and absorption processes for high separation capacities and low pressure drop. The performance of structured packing columns is highly depending on the interaction of gas and liquid flow phases inside the packing elements. As pointed out by Repke et al. (2007), understanding the complex flow behaviour in detail is crucial to improve on the prediction of separation performance. Packing materials are applied to intensify separation processes by supporting the spreading of the liquid phase in form of a thin film as uniformly as possible over the packing surface, while maintaining homogeneous counter-current gas flow distribution at low pressure drop. Thus, the features and dimensions of the packing geometry are the main determining parameters for the separation performance (Billet and Schultes, 1993). Comparisons of well-known packing materials demonstrate the importance of the optimal packing choice (e.g. Billet and Maćkowiak, 1988, Fischer et al., 2003). State of the art structured metal packing sheets are characterized by macro-structures, corrugations with a size of 0.01 to 0.03 m, and micro-structures, the textured surface with a typical feature size around a couple of a hundreds of millimetres (Zhao and Cerro, 1992). The macro-structure forms alternating channels offering a high specific surface area and low resistance to gas flow while also improving liquid and gas flow distribution. Several authors addressed the impact of the angle of inclination of the channels to the main flow direction and specific surface area on the column capacity and efficiency (Olujić et al., 2000, Olujić et al., 2004). Experiments of Bühlmann (1987) and Schultes (2008) on whole column scale show a significant positive influence of the micro-structure when comparing the performance of a structured packing with smooth or lamella like micro-structured surface. Many aspects can be considered causing the increase in mass transfer performance when using a micro-structured packing surface. Smaller scale studies, typically flow over inclined plate elements whose width is smaller 0.2 m, demonstrate that micro-structures may promote liquid wetting (Zhao and Cerro, 1992, Sebastia-Saez et al., 2013), stabilize the flow (Vlachogiannis and Bontozoglou, 2002) and can suppress recirculating eddies in the trough of the micro-structure as a consequence of resonance between the packing surface and waves on

the film surface (Tong et al., 2013). Moreover, Davies and Warner (1969) as well as Kohrt et al. (2011) find an increased liquid-side mass transfer in their experimental studies for micro-structured surfaces.

More in detail, Kohrt et al. (2011) scientifically proved that micro-structured surfaces intensify the liquid-side mass transfer for laminar and turbulent flow regimes compared to smooth surfaces independently from wetting conditions for the absorption of CO₂ in silicone oils on inclined plates. The enhancement of the mass transfer in this context is perhaps caused by the induction of fluid dynamic phenomena like cross mixing, near surface velocity gradients, recirculating regions and wave formations of the liquid film flow. Hence, Gerke et al. (2017) further investigated the velocity distribution of a film flow over a smooth and micro-structured inclined plate element and could indicate that micro-structures promote cross mixing perpendicular to the main flow direction of a liquid film flow. For a deeper understanding of the influence of real packing sheet geometry on fluid dynamics of the film flow, this paper now focuses on the investigation of film thicknesses and velocity distribution over the macro-structure of MONTZ-Pak B1-250 packing sheets with either a smooth surface or the original micro-structured surface. Therefore, a non-intrusive, optical μ -Stereoscopic-Particle-Imaging Velocimetry (μ SPIV)-method was developed to analyze the film flow from the backside through the corresponding solid surface using a molding of transparent polydimethylsiloxane (PDMS). Furthermore, the index of refraction of the liquid phase is matched to that of PDMS to avoid optical distortion at the liquid-solid interface. The results of this study can be used to validate computational fluid dynamic simulations and are the basis for an entire understanding of mass transfer processes in structured packings.

2. Experimental Set-up

The experimental set-up consists of a vertical measurement cell (see Figure 1) that holds the two different macro-structured PDMS moldings and ensures connections to a pulsation free gear pump driven liquid circuit. The liquid circuit is realized with a reservoir, pulsation buffer and thermostat to precondition the liquid entering the measurement cell over a multi-chamber overflowing weir that ensures evenly distributed film flow conditions at the top of the PDMS molding. After passing the 100 mm wide overflow weir, the liquid continues to flow gravity-driven along the macro-structures of the PDMS molding. The macro-structure was fully wetted for the presented liquid loads, while the gas phase was kept still inside the measurement cell. At the back of the PDMS molding and close to the field of view (FOV), a modulated window is installed together with a prism.

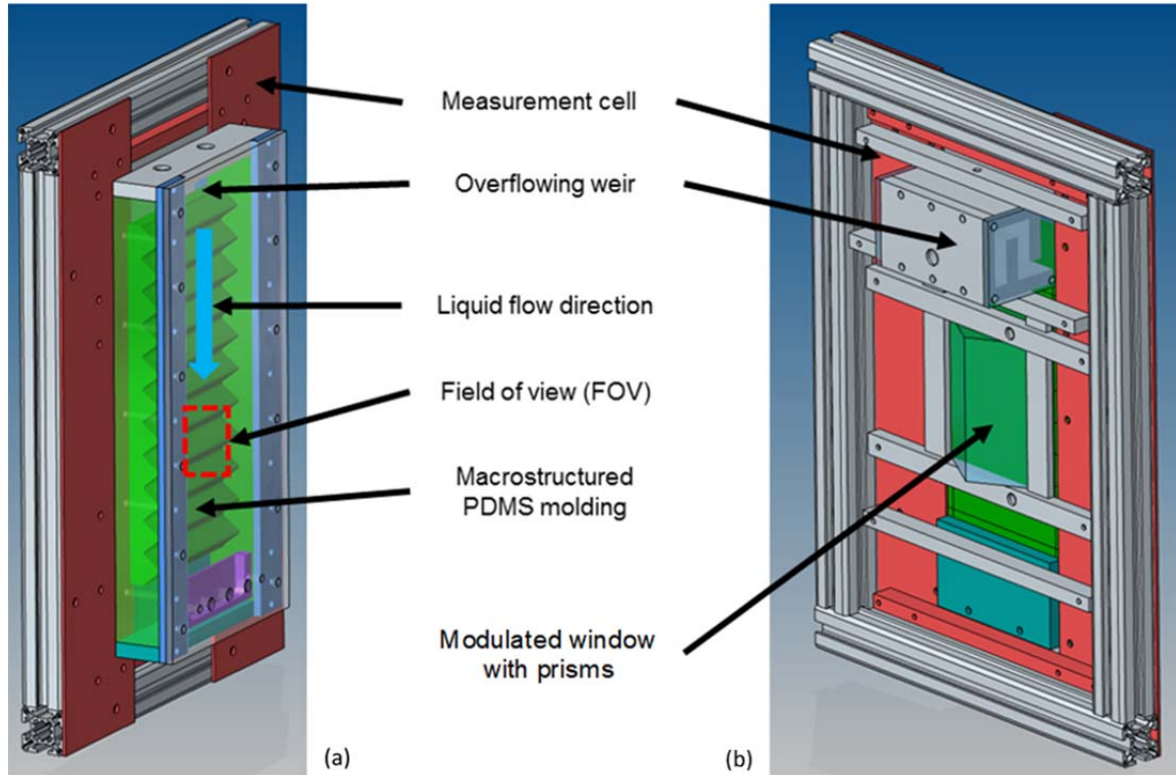


Figure 1: Measurement cell in front-view (a) and back-view (b) equipped with macro-structured PDMS molding.

The prisms are orientated to the camera positions regarding the stereoscopic angle of 45° to avoid optical distortions at the air-PDMS interface. Furthermore, the gap between the prism and the PDMS molding is filled up with clear liquid of the same refraction index like PDMS to avoid additional refractions.

Within the measurements an optically clear fluid-mixture consisting of glycerol (purity greater than 99.5 % in weight) and deionized water is used to match the refraction index of $RI = 1.41$, density of 1151 kg/m^3 and a surface tension of 26 mN/m . The resulting viscosity is estimated to 8.5 mPa s . During the experiments the temperature of the liquid entering the measurement cell was kept constant at 25°C .

A Stereoscopic Particle Image Velocimetry (SPIV) system (see Figure 2) is adapted for liquid film thicknesses smaller than 1 mm using zoom lenses and a micro calibration target (see Figure 3). SPIV allows to capture the three components of the velocity field inside the measurement plane by recording two-dimensional velocity fields with two cameras installed with a certain stereoscopic angle from two different perspective views. The third velocity component is reconstructed by perspective transformation during the post-processing. Hence, the μSPIV set-up thus enables visualization of spatial cross-mixing and eddy phenomena.

The μSPIV -system is realized using two sCMOS Andor HiSense Neo cameras (F) with a resolution of 5.5 MP together with two Navitar 12x Zoom Lens (E) as well as 570 nm longpass filters. The necessary zoom factors for measurements in micro-scale require extreme Scheimpflug-angles to ensure sharp particle images across whole field of view. Therefore, custom made Scheimpflug-adaptors has been designed and equipped. Furthermore, a 15 Hz double cavity 135 mJ Nd:YAG-Laser illuminates the measurement plane with 532 nm light sheets (A) perpendicular to the measurement cell surface. The cameras and laser are connected with a synchronizing unit to control the signal timing. The inserted $10 \mu\text{m}$ seeding particles (C) are coated with Rhodamine B resulting in a high signal-to-noise ratio for the measurements. The whole optical set-up is equipped on a 3D traverse system to change the FOV position with a repeatability of $40 \mu\text{m}$.

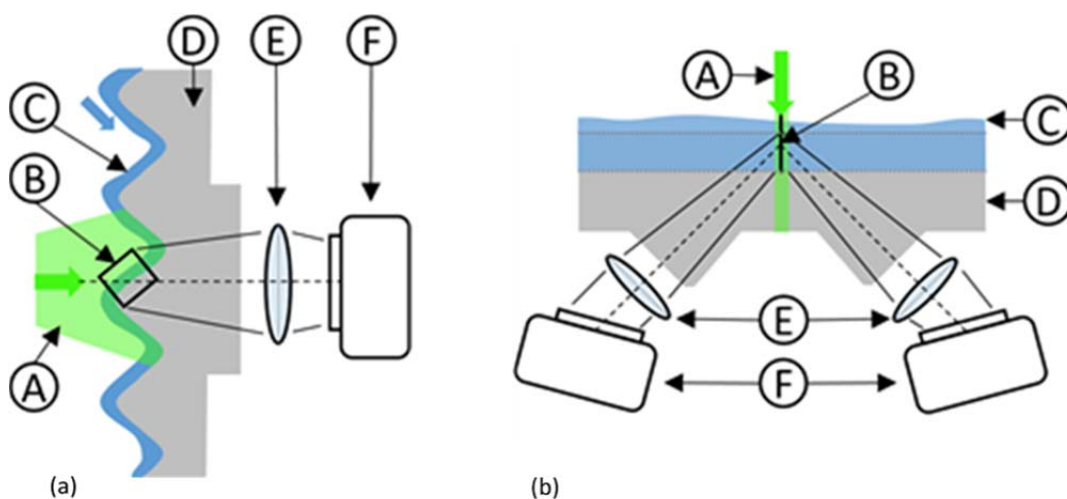


Figure 2: Optical setup for μSPIV measurements: side view (a), top view (b): A - light sheet, B - measurement plane, C - liquid with seeding, D - transparent macro packing geometry, E - microscope optics and Scheimpflug tilting adaptors, F - tilted cameras.

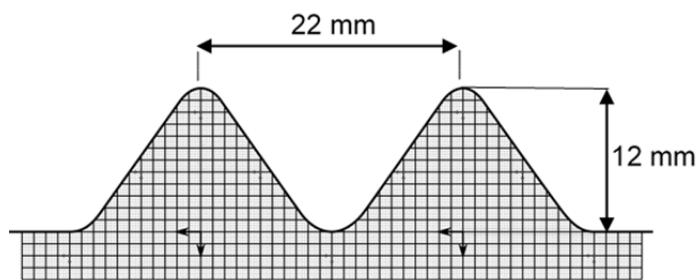


Figure 3: Custom calibration target with a $250 \mu\text{m}$ spaced grid. Thick lines indicate millimetre spacing.

The spatial distortion caused by the stereoscopic angle between both cameras is calibrated using a custom target with a double sided 250 μm spaced grid (see Figure 3). The grid is adjusted to the profile of the PDMS macro-structure and precisely aligned with the measurement plane (light sheets). A piezo stepper with 10 nm repeatability positions the calibration grid in several 100 μm steps along the horizontal z-axis.

During post-processing, the transformation between image and physical space is estimated using the volumetric calibration acquisitions. For each measurement, every camera acquired 100 double images that are post processed using Dantec Dynamic Studio v6.0. The displacement of particles images was kept smaller than 8 pixels to avoid loss of particle pairs when using interrogation areas of 32 pixel x 32 pixel by adjusting the inter-frame time accordingly. Each double frame resulted in a full adaptive-PIV algorithm accounting for velocity gradients was applied in combination with a wall mask to reduce zero velocity biasing.

3. Results

The experimental results provide a first comparison of the horizontal macro-structure of MONTZ-Pak B1-250 with a smooth or micro-structured surface for a Reynolds number of 20. The dimensions of the shown flow fields (Figures 4 and 5) measure 10 mm x 12 mm each. Figure 4 displays the velocity magnitude distribution on the investigated macro-structure for a smooth and micro-structured surface. Both measurements indicate low liquid velocities close to the wall and high velocities at the film surface in a similar range independently from the surface configuration. However, sufficiently lower velocities can be detected inside the valleys of the micro-structure (Figure 4(b)). The liquid velocities at the surface of the film flow are slightly higher for a smooth surface compared to the micro-structured surface.

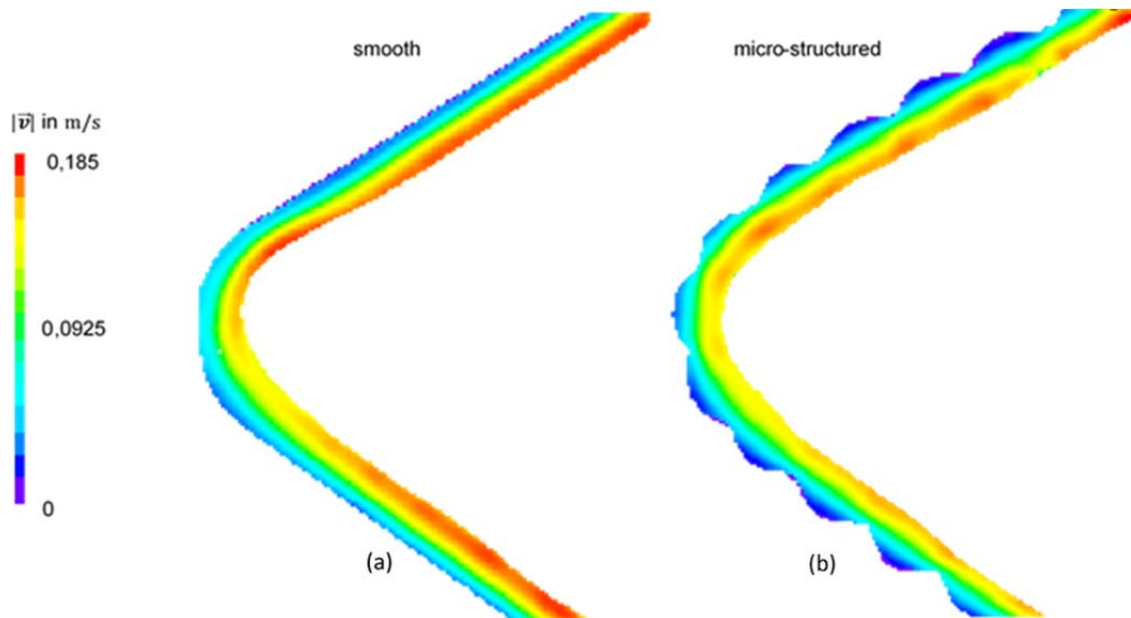


Figure 4: Measured velocity magnitude distribution on MONTZ-Pak B1-250 macro-structure with a smooth (a) and micro-structured (b) surface for glycerol/water mixture at $Re = 20$.

A comparison between the out-of-plane velocities (perpendicular to the measurement plane) in the liquid film for both surface configurations is presented in Figure 5. The out-of-plane velocity for a smooth surface is mostly close to zero across the whole film thickness at negative and positive sloped areas. Only within the turning point of the macro-structure, a slight increase of the out-of-plane velocity can be admitted. The results for the micro-structure surface indeed display higher out-of-plane velocities at numerous areas in both directions, which indicates a much more intense cross mixing occurrence in the liquid film compared to a smooth surface. This is in line with the findings of Gerke et. al. 2017 for an inclined, smooth and micro-structured plate. For this specific setup no recirculating region of the liquid film is observed as opposed to experiments of Negny et al. (2001) showing a jump in film thickness and recirculation on the positive incline of a smooth macro-structure as a consequence of decelerating film flow for similar Reynolds numbers. This difference could be explained by their measurement being located much farther downstream from the liquid inlet and a slightly different geometry of the macro-structure.

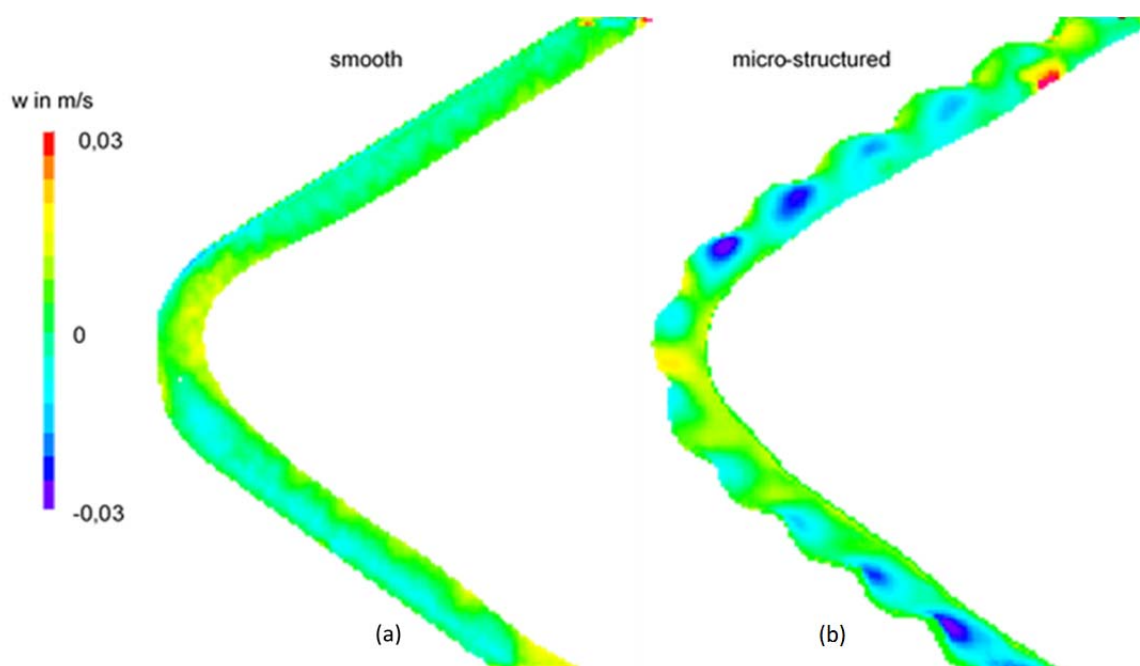


Figure 5: Out-of-plane velocity distribution on MONTZ-Pak B1-250 macro-structure with a smooth (a) and micro-structured (b) surface for glycerol/water mixture at $Re = 20$.

Figure 6 compares the velocity profiles across the film thickness at three different locations on the macro-structure. For a smooth surface, velocity profiles at the positive and negative inclined positions are similar across the height of the liquid film. Inside the turning point higher velocities are detected close to the wall and slightly lower values at the liquid film surface compared to the inclined positions. However, velocity profiles at all three positions are very similar for a micro-structured surface, whereas the effect inside the turning point is illustrated. For each measurement the position of the wall (PDMS-liquid interface) is defined by a distinct light intensity level for the mean of the acquired particle images. The turning point profiles indicate that this masking did not precisely estimated the wall position for this position as the near-wall profile, including the no-slip condition, is truncated. Also note that for PIV the near-wall velocity tends to be zero-biased when the borders of the rectangular interrogation areas do not align with the wall, which usually is the case due to the complex packing surfaces.

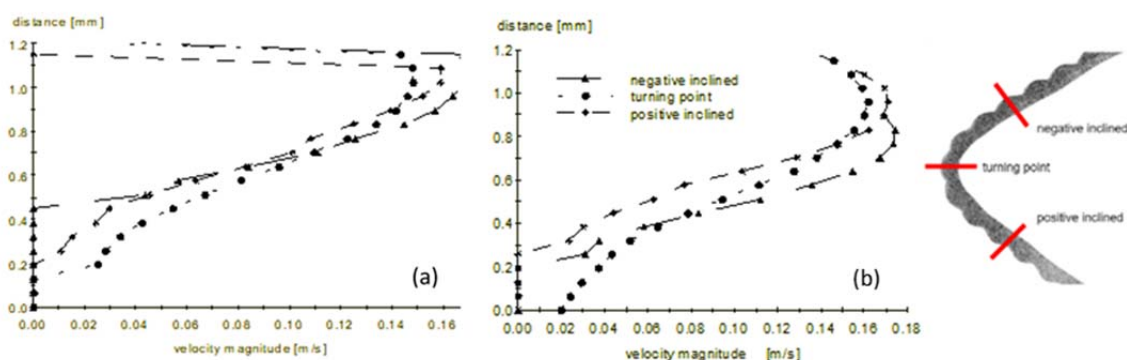


Figure 6: Velocity profiles across the film thickness at the middle of negative slope, turning point and the middle of the positive slope for smooth (a) and micro-structured (b) surface on MONTZ-Pak B1-250 for glycerol/water mixture at $Re = 20$.

4. Conclusions

This experimental study is the first to measure film thicknesses and 3D-velocity profiles of a liquid film flow on a real micro- and macro-structured packing geometry to gain understanding of fluid dynamics phenomena in structured packing columns on a micro-scale level.

Hence, velocity distribution measurements on a horizontal MONTZ-Pak B1-250 macro-structure with and without micro-structure were determined using a μ -Stereoscopic-Particle-Imaging Velocimetry. The results indicate a rather similar velocity magnitude distribution across the height of the liquid film independently from the surface conditions. However, the micro-structured surface induced a certainly higher cross-mixing appearance all over the liquid film.

Further investigations, especially for lower liquid loads, are necessary to cover industrial relevant fluid dynamic regimes. By traversing the SPIV system in small horizontal steps the time averaged volumetric flow field will be captured to reveal local effects of the micro-structure and macro-structure on the thin liquid film flow.

Acknowledgments

The authors kindly thank the German Research Foundation (DFG) for their financial support within the project RE-1705/8-2 and MONTZ for providing the packing materials.

References

- Billet, R., Maćkowiak, J., 1988, Application of modern packings in thermal separation processes, *Chemical engineering and technology*, 11(1), 213-227.
- Billet, R., Schultes, M., 1993, Predicting mass transfer in packed columns, *Chemical Engineering and Technology: Industrial Chemistry-Plant Equipment-Process Engineering-Biotechnology*, 16(1), 1-9.
- Bühlmann, U., 1987, Performance of Rombopak, Structured Column Packing, in *Distillation*, In *IChemESymp. No. 104, Distillation and Absorption*, 7.-9. Sept. 1987, A115-A127.
- Davies, J. T., Warner, K. V., 1969, The effect of large-scale roughness in promoting gas absorption, *Chemical Engineering Science*, 24(2), 231-240.
- Fischer, L., Bühlmann, U., Melcher, R. 2003, Characterization of high-performance structured packing, *Chemical Engineering Research and Design*, 81(1), 79-84.
- Gerke, S. J., Marek, A., Repke, J.-U., 2017, Untersuchung des Einflusses von Mikrostrukturen auf die Fluidynamik von Flüssigkeitsfilmströmungen auf Packungsoberflächen mithilfe von Stereo- μ PIV, 25th Symposium „Experimentelle Strömungsmechanik“, Karlsruhe/Germany, B 68.
- Kohrt, M., Ausner, I., Wozny G., Repke, J.-U., 2011, Texture influence on liquid-side mass transfer, *Chemical Engineering Research and Design*, Volume 89, Issue 8, 1405-1413.
- Negny, S., Meyer, M., Prevost, M. 2001, Study of a laminar falling film flowing over a wavy wall column: Part II. Experimental validation of hydrodynamic model, *International journal of heat and mass transfer*, 44(11), 2147-2154.
- Olujic, Z., Seibert, A. F., Fair, J. R., 2000, Influence of corrugation geometry on the performance of structured packings: an experimental study, *Chemical Engineering and Processing: Process Intensification*, 39(4), 335-342.
- Olujic, Z., Behrens, M., Colli, L., Paglianti, A., 2004, Predicting the efficiency of corrugated sheet structured packings with large specific surface area, *Chemical and Biochemical Engineering Quarterly*, 18(2), 89-96.
- Repke, J.-U., Ausner, I., Paschke, S., Hoffmann, A., Wozny, G., 2007, On the track to understanding three phases in one tower, *Chemical Engineering Research and Design*, 85(1), 50-58.
- Schultes, M., 2008, Raschig Super-Pak – Eine neue Packungsstruktur mit innovativen Vorteilen im Vergleich, *Chemie Ingenieur Technik*, 80(7): 927-933.
- Sebastian-Saez, D., Gu, S., Ranganathan, P., Papadakis, K., 2013, 3D modeling of hydrodynamics and physical mass transfer characteristics of liquid film flows in structured packing elements, *International Journal of Greenhouse Gas Control*, Elsevier BV, 492-502.
- Tong, Z., Marek, A., Hong, W., Repke, J.-U., 2013, Experimental and numerical investigation on gravity-driven film flow over triangular corrugations, *Industrial and Engineering Chemistry Research*, 52(45), 15946-15958.
- Vlachogiannis, M., Bontozoglou, V., 2002, Experiments on laminar film flow along a periodic wall, *Journal of Fluid Mechanics*, 457, 133-156.
- Zhao, L., Cerro, R. L., 1992, Experimental characterization of viscous film flows over complex surfaces, *International journal of multiphase flow*, 18(4), 495-516.